Hepatocyte Embryonic Ectoderm Development (Eed) Deficiency Causes Liver Injury, Fibrosis and Impacts Liver Regeneration

Yousra Ajouaou[1,2,*] and James Griffin[1,*], Sade Chaffatt[1], Charlene Chen[1], Martine McManus, and Kirsten C. Sadler[1,2,3]

[1] Program in Biology,
NYU Abu Dhabi,
PO Box 129188,
Abu Dhabi, United Arab Emirates

[2] Center for Genomics and Systems Biology,
NYU Abu Dhabi,
PO Box 129188,
Abu Dhabi, United Arab Emirates

[3]Corresponding author: ke27@nyu.edu

[*]These authors contributed equally to the work.

Summary

Regeneration depends on tightly coordinated transcriptional programs governed by a dynamic epigenetic landscape to regulate cell identity, proliferation, and tissue remodelling following injury. The liver's highly regenerative due to the ability to rapidly upregulate genes that drive the cell cycle and other genes important for regeneration. Trimethylation of histone 3 lysine 27 (H3K27me3) is deposited by the polycomb repressive complex 2 (PRC2) and many genes occupied by H3K27me3 in their promoters in uninjured livers become induced following PH. Here we test the hypothesis that depleting H3K27me3 by hepatocyte-specific deletion of Embryonic Ectoderm Development *(Eed^{HepKO})*, a key component of PRC2, changes the regenerative response in the liver. We show that Eed eliminates H3K27me3 in hepatocytes, resulting in reduced liver size, increased hepatocyte death, proliferation and fibrosis associated with upregulation of cell cycle and fibrogenic genes. Though these mice are less likely to survive two-thirds partial hepatectomy than wildtype controls, those that do survive increase liver mass faster than WTs. Importantly the genes that are occupied by H3K27me3 in control uninjured livers are upregulated in EED^{HepKO} and become further induced following PH. These data show that modulation of PRC2 activity disrupts epigenetic patterning, induces liver injury, and alters regenerative outcomes, suggesting that precise control of PRC2 function could be harnessed to enhance regenerative capacity.

Keywords

Liver regeneration, EED, H3K27me3, epigenetics, PRC2, mice, fibrosis

Introduction

Regenerating lost or damaged tissue is essential for all organisms to successfully mitigate injury. The field of regenerative medicine aims to promote regeneration by understanding and manipulating the cellular and molecular processes that govern tissue repair and regrowth. Epigenetic regulation of pro-regenerative genes is an attractive target to achieve these goals since epigenetic marks are reversible and can be altered by manipulating the complexes that write and erase them (Bell, 2024; Griazeva *et al*, 2023). To achieve this, it is important to determine which epigenetic modifications are the most important for regulating regeneration relevant genes.

While most tissues in mammals cannot regenerate, the liver is a notable exception. Following two-thirds partial hepatectomy (PH), or modest hepatocyte injury, the remaining hepatocytes reenter the cell cycle to restore liver mass (Michalopoulos & Bhushan, 2021). This process is dictated by a highly coordinated pattern of transcriptional changes that culminate in the synchronous progression of hepatocytes through the cell cycle. A leading hypothesis is that the uninjured liver, as well as other regeneration competent tissues, have an epigenetic prepattern which allows the pro-regenerative genes to be activated quickly in a precise, coordinated pattern following loss of liver mass or function. This is supported by recent studies from others (Cordero *et al*, 2024; Kawaguchi *et al*, 2024) and us (Zhang *et al*, 2021) that show uninjured, regeneration-competent tissues possess many pro-regenerative genes that are maintained in bivalent states marked by the repressive mark histone H3 lysine 27 trimethylated (H3K27me3) and H3K4me3. Our work also showed that H3K27me3 is lost from some of these genes during regeneration (Zhang *et al.*, 2021). Other supporting evidence from our previous studies show that that deleting the epigenetic regulator ubiquitin, PHD, and RING finger domain containing 1 (*Uhrf1*) in hepatocytes ($Uhrf1^{HepKO}$) accelerates liver regeneration in young mice (Wang *et al*, 2019), which is accompanied by global loss of H3K27me3 from promoters, which can enhance activation of pro-regenerative genes following PH. Together, these support the hypothesis that PRC2-mediated H3K27me3 occupancy of cell cycle and other proregenerative genes in hepatocytes sserves as the gatekeeper to their activation following liver injury

Previous studies have investigating the role of H3K27me3 in the liver via deletion of the PRC2 enzymatic factors, enhancer of zeste 1 or 2 (Ezh1, Ezh2), alone or in combination in hepatocytes show that there is redundancy in their function (Bae *et al*, 2015; Grindheim *et al*, 2019; Koike *et al*, 2014; Lau-Corona *et al*, 2020). The exception is when Ezh2 is knocked out in

hepatoblasts, which effectively depletes H3K27me3 and promotes acquisition of biliary identity (Yang *et al*, 2023) and reduces liver size(Koike *et al.*, 2014). While Ezh1 knockout mice have no discernible phenotype (REF) and Ezh2 knockout is embryonic lethal (O'Carroll *et al*, 2001), and therefore to study the function of PRC2 in the adult liver, investigators have used Ezh1 full-body knockout mice with a hepatocyte-specific knockout of Ezh2 using Cre recombinase driven by the hepatocyte specific albumin promoter (Alb:Cre; *Ezh1* $^{-/-}$ */Ezh2*^{HepKO}). These mice are viable, however, they develop multiple liver defects, including widespread cell death, severe fibrosis, susceptibility to liver damage including a failure to respond to PH or chemically mediated hepatocyte injury. These phenotypes are associated with a failure to induce genes which occupied by H3K27me3 in wild type (WT) livers (Bae *et al.*, 2015; Koike *et al.*, 2014). Interestingly, PRC2 was also implicated in acquisition of hepatocyte identity, suggested by the finding that *Ezh1* $^{-/-}$ */Ezh2*^{HepKO} postnatal mice had premature activation of hepatocyte identity genes (Grindheim *et al.*, 2019), which was further supported by other studies showing that Ezh2 deficiency early in development reduces biliary cell generation (Koike *et al.*, 2014; Yang *et al.*, 2023) . The fibrosis phenotype that developed in adult *Ezh1* $^{-/-}$*/Ezh2*^{HepKO} mice was attributed to the loss of bivalency on canonical fibrogenic genes, including *Tgfb1*, *Fbn1*, *Fstl1* and collagen, all of which are upregulated and shifted to active chromatin in *Ezh1* $^{-/-}$ */Ezh2*^{HepKO} livers (Grindheim *et al.*, 2019; Lau-Corona *et al.*, 2020; O'Carroll *et al.*, 2001). Finally, comparing male and female livers from this model show upregulation of female-specific genes in the male liver, and both sexes are more susceptible to hepatocyte damage (Lau-Corona *et al.*, 2020), suggesting that H3K27me3 mediates the sexual dimorphism of the hepatic transcriptome, including the induction of fibrogenic genes (Lau-Corona *et al.*, 2020). Together, these data show that loss of H3K27me3 deregulates multiple genes that are involved in hepatic identity, proliferative ability, survival and fibrogenesis. However, it remains unclear how PRC2 causes hepatocyte injury.

A major caveat of these studies is that they rely on whole-body deletion of Ezh1 combined with hepatocyte-specific loss of Ezh2 making it difficult to distinguish hepatocyte-intrinsic effects from contributions of other cell types. For example, PRC2 loss in hepatocytes could cause hepatocyte injury, while Ezh1 deficiency in non-hepatocyte populations could independently contribute to the observed fibrosis phenotype. An alternative target for cell specific elimination of PRC2 activity is through targeting Embryonic Ectoderm Development **(**Eed), a member of the PRC2 complex which functions to as a scaffolding protein that mediates PRC2's histone methylation activity via selective binding to DNA (REF). Full-body knockout of *Eed* is lethal in

zebrafish (Raby *et al*, 2021) and mice (Faust *et al*, 1995), and tissue specific Eed knock out has emerged as a useful tool to study the effect of Eed in several contexts (Casey-Clyde *et al*, 2025; Dauber *et al*, 2016; Ikeda *et al*, 2016; Koppens *et al*, 2016). Importantly, EED has emerged as a druggable target for epigenetic therapy, highlighting the importance of understanding how EED loss impacts different cell types to predict the tissue-level consequences of pharmacologic EED inhibition (Bashore *et al*, 2023; Chen *et al*, 2015; Shaliman *et al*, 2022; Zhao *et al*, 2022).

To further explore the effect of H3K27me3 loss specifically in hepatocytes, we evaluated mice with Eed loss in hepatocytes (Eed^{HepKO}). This effectively eliminated all H3K27me3 in hepatocytes of adult mice. While these mice appeared phenotypically normal, they had a reduced liver size associated with liver injury, cell death, proliferation, and fibrosis, similar to, but less severe than, Ezh1/2 deficient mice. We found that all genes marked with H3K27me3 in WT livers were induced in Eed^{HepKO} mice, and these were further upregulated following PH. Eed^{HepKO} mice had a lower survival following PH, but those that did survive had increased liver mass earlier than WTs. We conclude that examining PRC2 loss specifically in hepatocytes in order to distinguish hepatocyte-intrinsic regulatory responses from secondary effects arising from other liver cell types.

Results

Eed^{HepKO} mice are viable with depleted H3K27me3 in hepatocytes

We generated mice with a hepatocyte-specific knockout of *Eed* by crossing the Albumin:Cre transgenic line to a floxed allele of *Eed* with *loxP* sequences flanking exons 3 and 6; their offspring were further inbred to obtain Eed^{HepKO} mice. Qantitiative PCR (Figure 1A) Western blot analysis (Figure 1B) and immunofluorescence (Figure 1C) of the liver from 2 month old male Eed^{HepKO} mice showed effective depletion of Eed in hepatocytes. This resulted in the complete loss H3K27me3 (Figure 1D), thus confirming that these mice are useful for studying the role of PRC2 specifically in hepatocytes. Moreover, Eed^{HepKO} mice showed no gross phenotypic abnormalities compared to wildtype counterparts (Figure 1E) and continued to gain weight through 40 weeks (Figure 1F).

Eed loss reduces liver size and changes hepatic architecture

We evaluated the effect of Eed loss on the liver, and found 2-month-old male Eed^{HepKO} mice were smaller than WT (Figure 2A-B), though there was no apparent change in grows liver appearance in comparison to the strong fibrotic phenotype observed in $Ezh1^{-/-}/Ezh2^{HepKO}$ (Bae

et al., 2015; Grindheim *et al.*, 2019). Histological analysis of the livers revealed multiple abnormalities (Figure 2C), including increased number of blood vessels (Figure 2D), ductular reactions (20%), biliary fibrosis (20%), mitotic figures (20%), and signs of inflammation (60%), none of which pathologies were present in WT controls (Figure 2E). Therefore, loss of PRC2 specifically in hepatocytes causes changes to both hepatocytes and other hepatic cell types

Eed^{HepKO} changes the hepatic transcriptome

We predicted that the loss of PRC2 activity in hepatocytes have a direct effect on H3K27me3 regulated genes and, as a response to the phenotype caused by these changes, other genes would become deregulated through and indirect mechanism. To examine this, we carried out Bulk RNA sequencing of wildtype and *Eed*^{HepKO} livers from 2 month old male mice and found they had large differences, as shown by principal component analysis (Figure 3A). In *Eed*^{HepKO} mice livers, 2566 of the differentially expressed genes (DEGs) were upregulated and 411 were downregulated compared to wildtype livers (log2 fold change +/-1; padj <0.05; Figure 3B; Supplemental Table 1). Gene ontology (GO) analysis showed upregulated pathways were involved in tissue development, morphogenesis, an interesting contrast to the observed reduced liver size phenotype, and downregulation of metabolic and glycolytic pathways. (Figure 3C).
We next investigated which genes were regulated by H3K27me3 by evaluating the 1,076 genes occupied by H3K27me3 in promoters of WT livers (Zhang *et al.*, 2021), which were involved in processes related to transcription, growth factor activity and cell adhesion among other functions (Figure 3D; Supplemental Table 2). Of the 2,566 upregulated DEGs in *Eed*^{HepKO} livers, 354 were H3K27me3 enriched in WT mice (Figure 3E), but when we assessed expression of all H3K27me3-enriched genes, we see that nearly all either upregulated or nearly unchanged by the loss of PRC2 activity (Figure 3F). These were enriched for pathways associated with transcription and growth factor responses while (Figure 3G). We assume these are PRC2 targets that could be the cause of the *Eed*^{HepKO} phenotype. In contrast, the upregulated genes that are not H3K27me3 occupied were enriched for cell cycle genes, including those involved in chemotaxis and division (Figure 3G), suggesting these processes are activated as a response to the primary defects caused by PRC2 deficiency in hepatocytes.

Eed^{HepKO} liver transcriptome resembles that of *Ezh1/2*^{HepKO} livers

The phenotype of *Eed*^{HepKO} mice is reminiscent of the *Ezh1*$^{-/-}$*/Ezh2*^{HepKO} mice and we further investigated transcriptomes of these two models. While there were 1226 DEGs shared between both samples, there were 1,751 and 1,250 DEGs unique the *Eed*^{HepKO} and *Ezh1*$^{-/-}$*/Ezh2*^{HepKO}

samples, respectively (Figure 4A; Table S3) and the expression of genes in the unified set of genes were have the same expression pattern, albeit with subtle differences (Figure 4B). DEG's common to both sets were related to cell differentiation and metabolic processes (Figure 4C). DEG's unique to the *Ezh1/2*^{HepKO} mice were enriched in functions related to glycolysis and cell respiration (Figure 4D), while DEG's unique to the *Eed*^{HepKO} mice were primarily involved in cell proliferation and inflammation, including mitotic genes, cell cycle regulation, wound healing, and DNA replication. Several studies have shown that fibrogenic genes are upregulated in *Ezh1*$^{-/-}$ */Ezh2*^{HepKO} livers. We therefore investigated these genes in *Eed*^{HepKO} samples and found that while they were all induced, the magnitude of induction was less than in the double knockout (Figure 4F). Therefore, while both models have PRC2 loss-of-activity have transcriptional response indicating liver damage and fibrosis, the effects are not identical and the *Eed*^{HepKO} mice have a specific deregulation of genes involved in proliferation.

Hepatic EED loss increases liver damage, cell proliferation, and fibrosis

We next investigated the phenotypes associated with the transcriptional changes observfed in *Eed*^{HepKO} mice. We found that serum levels of alanine aminotransferase (ALT) and aspartate aminotransferase (AST) levels were significantly increased roughly three-fold in *Eed*^{HepKO} mice, reflecting liver damage (Figure 5A). This was accompanied by an increase in TUNEL labeled cells as an indicator of cell death in *Eed*^{HepKO} livers (Figure 5B). Transcriptomic analysis indicated that the genes involved in fibrosis were induced in *Eed*^{HepKO} livers, albeit at a reduced level compared to *Ezh1*$^{-/-}$ */Ezh2*^{HepKO} livers. Sirius Red staining as a marker of fibrosis was significantly increased in *Eed*^{HepKO} livers as were all of the canonical fibrosis related genes, the majority of which were not marked by H3K27me3 in WT livers (Figure 5D). GO analysis identified mitotic cell cycle pathways induced in *Eed*^{HepKO} livers and we therefore investigated the expression of the entire cell proliferation canonical geneset and found all to be induced (Figure 5E). This was reflected in the detection of increased markers for mitotic cells (phosphor-histone H3) and the proliferation marker, ki67 (Figure 5F). Interestingly histological analsyis of the mitotic figures showed several appeared to be abnormal, with lagging chromosomes and multipolar spindles (Figure 5G). This suggests that PRC2 deficiency in hepatocytes causes upregulation of most genes suppressed by H3K27me3 in WT livers, leading to hepatocyte damage and death and pro-fibrogenic signals, with fibrosis and reactive proliferation as a secondary response.

***Eed*^{HepKO} mice have divergent responses to PH**

The liver damage and fibrosis in *Eed*^{HepKO} livers suggests that, like *Ezh1* $^{-/-}$*/Ezh2*^{HepKO} mice (Bae *et al.*, 2015; Lau-Corona *et al.*, 2020), they would be unable to regenerate. However, H3K27me3 levels were reduced during regeneration of WT mice (Zhang *et al.*, 2021) and remained absent in *Eed*^{HepKO} mice (Figure 6A) at time points when proliferation genes are induced. This suggests removal of repression by H3K27me3 as mechanism that regulates regeneration relevant genes. Notably, while all WT mice survived PH, only 64% of the *Eed*^{HepKO} mice survived (Figure 6B), similar to the high mortality observed in *Ezh1* $^{-/-}$*/Ezh2*^{HepKO} mice challenged to regenerate (Bae *et al.*, 2015). Interestingly, the *Eed*^{HepKO} mice that did survive, however, recovered liver mass faster than WT controls, as measured by their liver/body weight ratio (Figure 6C). Bulk RNAseq analysis over the regenerative time course of WT and *Eed*^{HepKO} mice after PH showed that while some of the H3K27me3-marked genes were downregulated during regeneration in WT livers, most were induced. The profile in *Eed*^{HepKO} livers was strikingly different, with all these targets being overexpressed in uninjured livers, then downregulated at 30 hours after PH and nearly all highly expressed at 40 and 48 hours after PH, time points when cells proceed from S phase to mitosis, (Figure 5D). Interestingly, the genes that were differentially expressed in *Eed*^{HepKO} lives compared to WT at 40 hours after PH, the time point when many of the pro-regenerative genes are upregulated in controls (Wang *et al.*, 2019; Zhang *et al.*, 2021) were mostly involved in development and cell division, whereas the downregulated genes were canonical hepatocyte metabolic functions (Figure 5E). This suggests that PRC2 loss causes hepatocyte damage which impairs liver regeneration in some mice, while those that survive are able to compensate, upregulated proliferative genes and increase liver mass.

Discussion

Liver development and regeneration rely on tightly regulated epigenetic patterning to control and enact genetic code for proper gene expression and the production of healthy tissue. However, it is unknown why the liver may utilize these regenerative genes as opposed to virtually all other tissues in the body despite sharing the same genome. Investigation of these epigenetic processes is thus vital to the understanding of the hepatic regenerative process and how it could be enabled in other tissues. Polycomb repressive complex 2 (PRC2) enables one such epigenetic process that selectively represses genes to promote healthy tissue development, specifically the trimethylation of histone 3 lysine 27 (H3K27me3). Previous experimental work aimed at understanding PRC2's role has focused on disabling the enzymatically active proteins in PRC2, the relatively interchangeable EZH1 and EZH2 proteins, though they require a complex knockdown of multiple proteins, both in the liver and throughout

the body, to produce viable embryos and may not accurately reflect the activity of PRC2 in the liver alone. EED is a constituent protein of PRC2 that allows it to selectively bind DNA sequences and promote gene silencing; as with the enzymatically active proteins, EZH1 and EZH2, EED is required for PRC2 function. The hepatocyte-specific knockdown of EED, as opposed to the complicated double-knockdown of EZH1 and EZH2, is thus an attractive and cleaner approach to understanding PRC2 and the genetic regulation of regeneration.

PRC2 activity is required for embryo viability, both in mice and zebrafish, so we were surprised that mice lacking hepatic PRC2 function via EED knockdown produced superficially normal progeny. Even at 2 months of age, *Eed*^{HepKO} mice thrived and their livers did not display the severe fibrosis seen in the *Ezh1/2*^{HepKO} strain. Upon deeper investigation, we observed a similar yet milder phenotype in the *Eed*^{HepKO} mice seen in the *Ezh1/2*^{HepKO} strain: livers of *Eed*^{HepKO} mice were chronically damaged. Present abnormalities included an increased number of blood vessels and bile ducts, actively dividing cells, inflammation, and fibrosis. Despite the visible physical changes, there was no obvious source of the damage, motivating us to perform bulk RNAseq on these livers to assess expression changes that may produce or indicate the source of this damage. Indeed, the loss of hepatocellular H3K27me3 broadly disrupted the transcriptomes of their livers including, but not limited to, genes known to be enriched with H3K27me3. Pathway association of these genes indicated that PRC2-associated genes regulated processes related to transcription, growth factor activity, and cell adhesion, while the other genes were enriched for cell cycle activity. We believe that the PRC2-associated genes are responsible for the observed liver phenotype, while the non-H3K27me3-enriched genes are a response to the resulting damage. When compared to XX

With the established characterization of the liver tissue phenotype, transcriptome changes, and identification of increased cell cycle activity in the *Eed*^{HepKO} mice and how it compares to that of the *Ezh1/2*^{HepKO} mice, we decided to test the *Eed*^{HepKO} mouse response to two-thirds partial hepatectomy (PHx). *Ezh1/2*^{HepKO} mice were not able to recover and regeneration from PHx, which was attributed to the loss of hepatic PRC2 activity. Given the similar loss of hepatic H3K27me3 markers yet milder phenotype in *Eed*^{HepKO} mice compared to *Ezh1/2*^{HepKO} mice, we hypothesized that *Eed*^{HepKO} mice could potentially regenerate more successfully than the *Ezh1/2*^{HepKO} mice. Not only did *Eed*^{HepKO} mice survive PHx at a higher rate than *Ezh1/2*^{HepKO} mice, they regenerated faster than wildtype mice as quantified by their liver-to-body mass ratio starting around 30-40 hours post-PHx. As regeneration requires the rapid reactivation of many genes via the removal of numerous epigenetic silencing markers, including H3K27me3, we

speculate that *Eed*^{HepKO} mice are primed for regeneration as many regenerative genes are already open to transcription.

Our data thus demonstrates that the removal of the H3K27me3 epigenetic marker via PRC2 deactivation in hepatocytes induces liver injury, alters the hepatic transcriptome, and may promote liver regeneration, indicating that the precise control of PRC2 function is a key player in modulating and potentially enhancing regenerative capacity.

Data and Code availability

Raw data (fastq files) and processed files (raw counts) for bulk RNAseq have been deposited in GEO as GEO: XXX. All are publicly available as of the date of publication. This paper does not report original code.

Acknowledgments

This work was supported by the NYUAD Faculty Research Fund (AD188), NIH (2R01DK080789-12A1) to KCS, and Tamkeen under the NYU Abu Dhabi Research Institute Award to the NYUAD Center for Genomics and Systems Biology (ADHPG-CGSB13). All imaging was carried out in the NYUAD Core Technology Platform Imaging facility with expert support by Rashid Razgui. RNAseq bulk libraries were performed by NYUAD Core Technology Platform Imaging with the expert help of Marc Arnoux and bioinformatics assistance from the NYUAD Bioinformatics Core. We are grateful for Sirius Red staining by Elena Magnani, TUNEL staining by Balnur Ibraesh and the technical support during collaboration with the Halder Lab (KU-Leuven). We appreciate the expertise of Nizar Drou for assistance with bulk RNAseq. We are thankful to all Sadler lab members for valuable discussions.

Author contributions

JG, YA, and KCS conceptualized the project, JG, YA, SC, CC, MM, and KCS developed the methodology, JG, YA, CC, MM, KCS carried out the analysis, JG, YA, SC, and MM carried out the investigation, JG, YA, SC, CC, and KCS created the visualization, KCS provided resources, KCS provided supervision, project administration, JG, YA, and KCS wrote the manuscript. JG, YA, CC, and KCS reviewed and edited the manuscript.

Declaration of interests

The authors declare no competing interests.

Supplemental information titles and Legend

Document S1. XX

Supplemental Table S1. XX

Figure Legends

Figure 1. Hepatocyte-specific loss of EED is well-tolerated

A. qPCR analysis of *Eed* mRNA expression in 2-month-old, male wild-type and *Eed*^{HepKO} mouse livers and kidneys. **B.** Western Blot analysis comparing the presence of EED in 2-month-old, male wildtype, *Eed*^{Het}, and *Eed*^{HepKO} mouse livers. **C.** Immunofluorescent imaging of EED and nuclei in 2-month-old, male wildtype and *Eed*^{HepKO} mice. **D.** Western Blot analysis comparing the presence of H3K27me3 in 2-month-old, male wild-type, *Eed*^{Het}, and *Eed*^{HepKO} mice livers and kidneys. **E.** Representative images of 2-month-old, male wild-type and *Eed*^{HepKO} mice. **F.** Body weight measurements of male wild-type and *Eed*^{HepKO} mice between 5 and 40 weeks of age. Data are representative of at least two independent experiments with n = 2-3 (A-D), n = 5-6 (F) per group. Values are presented as the mean ± SD and were compared by two-tailed unpaired Student's t-test (A) and by two-way ANOVA with Bonferroni's multiple comparisons test. Significant differences are indicated as follows: ns p>0.05, *p<0.05, **p<0.01, ***p<0.001, ****p<0.0001.

Figure 2. Hepatic loss of EED affects liver size and vascular structure

A. Representative images of 2-month-old, male wildtype and *Eed*^{HepKO} mouse livers. **B.** Body-to-liver weight ratios between 2-month-old, male wildtype and *Eed*^{HepKO} mice (n = ; P-value). **C.** Representative H&E-stained histological images of 2-month-old, male wild-type and *Eed*^{HepKO} mouse livers at 10X and 40X magnification. **D.** Quantification of number of vessels and ducts present in randomly selected 40X magnification images of wildtype and *Eed*^{HepKO} mice. **E.** Table of pathologies present in the wild-type and *Eed*^{HepKO} mice. Data are representative of at least two independent experiments with n = 6-14 (B) per group. Values are presented as the mean ± SD and were compared by two-tailed unpaired Student's t-test (B). Significant differences are indicated as follows: ns p>0.05, *p<0.05, **p<0.01, ***p<0.001, ****p<0.0001.

Figure 3. *Eed*^{HepKO} liver transcriptome is disrupted

A. PCA plot comparing the liver transcriptomes of 2-month-old, male wild-type and *Eed*^{HepKO} mice. **B.** Volcano plot of upregulated and downregulated genes (FDR<0.05 and log2FC>1). **C.** GO pathways analysis of genes upregulated and downregulated in *Eed*^{HepKO} mice. **D.** xx. **E.** Venn diagram comparing the upregulated genes in *Eed*^{HepKO} mice and the list of known H3K27me3-enriched genes. **F.** Heat map of gene expression of H3K27me3-enriched genes in 2-month-old, male wild-type and *Eed*^{HepKO} mice. **G.** GO analysis of all upregulated genes in

Eed^{HepKO} mice. **H.** GO analysis of upregulated genes in *Eed*^{HepKO} mice that are known to be enriched with H3K27me3.

Figure 4. Enhanced hepatic cell cycle response in *Eed*^{HepKO} vs. *Ezh1/2*^{HepKO} livers

A. Venn diagram of differentially expressed genes in *Eed*^{HepKO} and *Ezh1/2*^{HepKO} mouse livers. **B.** xx. **C.** Gene ontology analysis of genes that are differentially expressed in both *Eed*^{HepKO} and *Ezh1/2*^{HepKO} mouse livers, as well as those only differentially expressed in **D.** *Ezh1/2*^{HepKO} mouse livers or in **E.** *Eed*^{HepKO} mouse livers.

Figure 5. Hepatic EED loss causes liver damage and increases cell proliferation and fibrosis

A. Serum ALT and AST concentrations in 2-month-old, male wild-type and *Eed*^{HepKO} mice (n = 3; P-values). **B.** Immunofluorescent imaging and quantification of TUNEL (n = ; P-value). **C.** Representative Sirius Red/Fast Green-stained histological images of 2-month-old, male wild-type and *Eed*^{HepKO} mouse livers at 3X and 40X magnification and quantification of stain (n = ; P-value). **D.** Heat map of expression and **E.** quantification of fibrosis-related genes and **F,G.** cell cycle-related genes in 2-month-old, male wild-type and *Eed*^{HepKO} mouse livers (n = 5). **H.** Mitotic figures present in *Eed*^{HepKO} mouse livers. **I.** Representative immunofluorescent images and quantification of proliferation markers, phosphor H3 and ki67, in 2-month-old, male wild-type and *Eed*^{HepKO} mouse livers (n = ; P-value).

Figure 6. EedHepKO mice show enhanced liver regeneration

A. Western blot analysis of H3K27me3 and Histone 3 at select time points in wildtype and *Eed*^{HepKO} mouse livers following two-thirds partial hepatectomy and **B.** subsequent quantification of H3k27me3 marker relative to Histone 3 (n = ; P-value). **B.** Visualization of mouse genotype vs. two-thirds partial hepatectomy survival. **C.** Quantification of regeneration rate in mice following two-thirds partial hepatectomy via liver-to-body weight ratios at select time-points (n = ; P-value). **D.** Heat map of H3K27me3-enriched gene expression in *Eed*^{HepKO} mouse livers via bulk RNAseq before and after two-thirds partial hepatectomy. **E. XX**

Materials and Methods

Generation of *Eed*^{HepKO} mice

Mouse husbandry and care was conducted according to the New York University Abu Dhabi (NYUAD) Institutional Animal Care and Use Committee (IACUC) protocol 23-0011A. Mice were weaned at 21-days-old and fed *ad libitum*.

C57BL/6J mice were purchased from The Jackson Laboratory: wildtype mice, transgenic mice possessing Cre under the expression of the albumen promoter ("Alb:Cre"), and targeted mutant mice with *loxP* sites flanking exons 3 and 6 of the embryonic ectoderm development (*Eed*) gene ("Eed^{flox}"; strain #022727). Alb:Cre and Eed^{flox} mice strains were crossed and further inbred to produce "*Eed*^{HepKO}" mice that lack functional EED in hepatocytes. Genotyping was performed by Transnetyx, Inc. (Cordova, TN) via polymerase chain reaction on mouse tail clippings obtained when weaned at 21-days-old.

Partial Hepatectomy

Partial hepatectomy (PH) was performed as described by Mitchell et al. (Mitchell and Willenbring, 2008). Male mice aged 8–12 weeks were anesthetized with isoflurane (5% for induction followed by 1.5–2% for maintenance) between 08:00 am and 12:00 pm to minimize circadian variability. After induction of anesthesia, mice were weighed and placed on a sterile surgical field. A midline abdominal incision (~3 cm) was made to expose the liver, followed by opening of the peritoneal cavity. The falciform ligament was transected and a two-thirds hepatectomy was performed by ligating and resecting the left lateral and median lobes using 4-0 silk sutures (Assut Sutures, L4553WF). The peritoneal cavity was closed with 4-0 sutures (Assut Sutures, L4553WF), and the skin was closed with wound clips (BrainTree Scientific, EZC APL). Mice were euthanized at 30, 40, or 48 hours following surgery. For measuring the weight of the regenerating liver following surgery, only the intact, non-resected lobes were measured. Tissue samples were snap-frozen in liquid nitrogen and stored at -80 °C for downstream analyses.

Western blotting

Protein was extracted from mouse tissue stored at -80°C using T-PER™ Tissue Protein Extraction Reagent (Thermo Scientific) supplemented with protease inhibitor cocktail (Roche), and the tissue lysate was cleared via centrifugation. Protein concentration was quantified via Qubit™ assay. Extracted protein was mixed with 4X Laemmli buffer (BioRad), briefly boiled, spun to remove insoluble content, cooled, and loaded into a 10% acrylamide/bisacrylamide denaturing gel. Voltage was initially set to 40V to allow for uniform entry into the gel, at which

point the voltage was raised to 100V. Proteins were transferred to a PVDF membrane at 300mA for 1.5 hours on ice. Membrane was blocked for 1 hour at room temperature with TBS (BioRad) supplemented with 0.1% Tween-20 (Sigma Aldrich) containing 5% skim milk (Sigma Aldrich), incubated overnight at 4 °C with 1: 1000 primary antibody diluted in blocking solution (EED, Cell-Signaling, Cat. No. 51673S; H3K27me3, Active Motif, Cat. No. 61017; H3, Santa Cruz, Cat. No. 10809) followed by secondary antibody diluted 1: 2500 in blocking solution (HRP-conjugated anti-Rabbit or anti-Mouse, Promega). Chemiluminescence was revealed with ECL Clarity (BioRad) and imaged with ChemiDoc MP Imaging System (BioRad).

Immunofluorescence

Mouse liver tissue was resected and fixed in 10% neutral-buffered formalin (Sigma Aldrich) at 4°C for 24-48 hours. Tissue was cryopreserved by incubation in 30% sucrose in PBS overnight, followed by mounting in OCT (Leica Biosystems) and frozen with dry ice. 14 μm cryosections were used for immunofluorescence. Sections were rehydrated with PBS, permeabilized with 1% Tween-20 (Sigma Aldrich) in PBS for 5 minutes, and blocked with 2.5% BSA (Sigma Aldrich) and 0.1% Triton X-100 (XX) in PBS for 1 hour. Primary antibody was dissolved 1:200 in blocking buffer and incubated for 3 hours. After washing the sections, secondary antibody was dissolved 1:400 in blocking buffer and incubated for 1 hour. Sections were then washed with PBS and mounted in Vectashield containing DAPI (Vector) for imaging. Imaging was performed on a Leica Stellaris 8 Confocal Microscope and quantified with LasX software.

Histology

Mouse liver tissue was resected and fixed in 10% neutral-buffered formalin (Sigma Aldrich) at 4°C before mounting into paraffin blocks. Sections of the blocks were deparaffinized in xylene, rehydrated, and stained/counterstained with either hematoxylin/eosin or Sirius Red/Fast Green. Stained sections were then dehydrated and mounted. Imaging was performed on a DSX2000 Digital Microscope (Evident Scientific) and quantified with PRECi software.

Alanine aminotransferase/AST serum analysis

Blood was collected from mice via retro-orbital bleeding. After allowing the blood to clot for 30 minutes at room temperature, blood was centrifuged at 1,000 x G for 10 minutes, and the top serum layer was collected and frozen at -80°C for later analysis. ALT and AST concentrations were measured using the Mouse ALT ELISA Kit (Abcam) or the Mouse AST ELISA Kit (Abcam), respectively, and were plotted for visualization with Graphpad Prism 10.

TUNEL staining

14 μm cryosections of mouse liver tissue were prepared as described above. Cell death was assessed using the In Situ Cell Death Detection Kit, Fluorescein or TMR Red (REF 11684795910/12156792910; Roche). In brief, cryosections were washed with PBS for 30 minutes and permeabilized with 0.1% Triton X-100 (XX) and 0.1% sodium citrate (XX) for 2 minutes. Per the manufacturer's instructions, sections were washed with PBS an additional 2 times, incubated with the kit-provided TUNEL reaction mixture for 60 minutes at 37°C, and washed 3 times with PBS. Sections were mounted in Vectashield containing DAPI (Vector) for imaging. Imaging was performed on a Leica Stellaris 8 Confocal Microscope and quantified with LasX software.

Sequencing library preparation and bulk RNA-seq analysis

Livers were resected from 2-month-old Wild-type and Eed^{HepKO} mice either before or after partial hepatectomy and stored at -80°C. Tissue was homogenized in 500 ml of Trizol (Thermo Fisher Scientific) in a Dounce homogenizer. RNA was isolated using column extraction on a QIAGEN RNeasy Mini Kit (Qiagen, 74104) in tandem with on-column DNase I digestion (Qiagen, 79254) as per the manufacturer's instructions. RNA was quantified on a QubitTM fluorometer and quality-checked on an Agilent TapeStation. 1000 ng of total RNA was subsequently used to prepare RNA-seq library by using TruSeq RNA sample prep kit (Illumina) according to the manufacturer's instructions. Paired-end RNA-sequencing was performed on a NovaSeq 6000 (Illumina) (CTP-NYUAD, Abu Dhabi, UAE). Sequenced reads were aligned to the mouse genome (mm10), and uniquely mapped reads were used to calculate gene expression. Data analysis was performed using R program (DESeq2 package). Differentially expressed genes are considered significant when the false discovery rate (FDR or adjusted p-value) < 0.05 and the log2 fold change (log2FC) > 1. All RNA-seq analyses were performed using ≥2 biological replicates.

Statistical analysis

All statistical tests, error bars, and N numbers are reported in the corresponding figure legends with p-values indicated in the figure when significant. All statistical analyses were conducted using GraphPad Prism (GraphPad Software). XX need add quantification method

References

Bae WK, Kang K, Yu JH, Yoo KH, Factor VM, Kaji K, Matter M, Thorgeirsson S, Hennighausen L (2015) The methyltransferases enhancer of zeste homolog (EZH) 1 and EZH2 control hepatocyte homeostasis and regeneration. *FASEB J* 29: 1653-1662

Bashore FM, Foley CA, Ong HW, Rectenwald JM, Hanley RP, Norris-Drouin JL, Cholensky SH, Mills CA, Pearce KH, Herring LE *et al* (2023) PROTAC Linkerology Leads to an Optimized Bivalent Chemical Degrader of Polycomb Repressive Complex 2 (PRC2) Components. *ACS Chem Biol* 18: 494-507

Bell CG (2024) Epigenomic insights into common human disease pathology. *Cell Mol Life Sci* 81: 178

Casey-Clyde T, Liu SJ, Pelonero A, Serrano JAC, Teng C, Jang Y-G, Vasudevan HN, Padmanabhan A, Bush JO, Raleigh DR (2025) Eed controls craniofacial osteoblast differentiation and mesenchymal proliferation from the neural crest. *eLife* 13: RP100159

Chen H, Gao S, Li J, Liu D, Sheng C, Yao C, Jiang W, Wu J, Chen S, Huang W (2015) Wedelolactone disrupts the interaction of EZH2-EED complex and inhibits PRC2-dependent cancer. *Oncotarget* 6: 13049-13059

Cordero J, Elsherbiny A, Wang Y, Jürgensen L, Constanty F, Günther S, Boerries M, Heineke J, Beisaw A, Leuschner F *et al* (2024) Leveraging chromatin state transitions for the identification of regulatory networks orchestrating heart regeneration. *Nucleic Acids Res* 52: 4215-4233

Dauber KL, Perdigoto CN, Valdes VJ, Santoriello FJ, Cohen I, Ezhkova E (2016) Dissecting the Roles of Polycomb Repressive Complex 2 Subunits in the Control of Skin Development. *J Invest Dermatol* 136: 1647-1655

Faust C, Schumacher A, Holdener B, Magnuson T (1995) The eed mutation disrupts anterior mesoderm production in mice. *Development* 121: 273-285

Griazeva ED, Fedoseeva DM, Radion EI, Ershov PV, Meshkov IO, Semyanihina AV, Makarova AS, Makarov VV, Yudin VS, Keskinov AA *et al* (2023) Current Approaches to Epigenetic Therapy. *Epigenomes* 7

Grindheim JM, Nicetto D, Donahue G, Zaret KS (2019) Polycomb Repressive Complex 2 Proteins EZH1 and EZH2 Regulate Timing of Postnatal Hepatocyte Maturation and Fibrosis by Repressing Genes With Euchromatic Promoters in Mice. *Gastroenterology* 156: 1834-1848

Ikeda K, Ueda T, Yamasaki N, Nakata Y, Sera Y, Nagamachi A, Miyama T, Kobayashi H, Takubo K, Kanai A *et al* (2016) Maintenance of the functional integrity of mouse hematopoiesis by EED and promotion of leukemogenesis by EED haploinsufficiency. *Sci Rep* 6: 29454

Kawaguchi A, Wang J, Knapp D, Murawala P, Nowoshilow S, Masselink W, Taniguchi-Sugiura Y, Fei JF, Tanaka EM (2024) A chromatin code for limb segment identity in axolotl limb regeneration. *Dev Cell* 59: 2239-2253 e2239

Koike H, Ouchi R, Ueno Y, Nakata S, Obana Y, Sekine K, Zheng YW, Takebe T, Isono K, Koseki H *et al* (2014) Polycomb group protein Ezh2 regulates hepatic progenitor cell proliferation and differentiation in murine embryonic liver. *PLoS One* 9: e104776

Koppens MA, Bounova G, Gargiulo G, Tanger E, Janssen H, Cornelissen-Steijger P, Blom M, Song JY, Wessels LF, van Lohuizen M (2016) Deletion of Polycomb Repressive Complex 2 From Mouse Intestine Causes Loss of Stem Cells. *Gastroenterology* 151: 684-697 e612

Lau-Corona D, Bae WK, Hennighausen L, Waxman DJ (2020) Sex-biased genetic programs in liver metabolism and liver fibrosis are controlled by EZH1 and EZH2. *PLoS Genet* 16: e1008796

Michalopoulos GK, Bhushan B (2021) Liver regeneration: biological and pathological mechanisms and implications. *Nature Reviews Gastroenterology & Hepatology* 18: 40-55

O'Carroll D, Erhardt S, Pagani M, Barton SC, Surani MA, Jenuwein T (2001) The polycomb-group gene Ezh2 is required for early mouse development. *Mol Cell Biol* 21: 4330-4336
Raby L, Völkel P, Hasanpour S, Cicero J, Toillon R-A, Adriaenssens E, Van Seuningen I, Le Bourhis X, Angrand P-O (2021) Loss of Polycomb Repressive Complex 2 Function Alters Digestive Organ Homeostasis and Neuronal Differentiation in Zebrafish. *Cells* 10: 3142
Shaliman D, Takenobu H, Sugino RP, Ohira M, Kamijo T (2022) The PRC2 molecule EED is a target of epigenetic therapy for neuroblastoma. *Eur J Cell Biol* 101: 151238
Wang S, Zhang C, Hasson D, Desai A, SenBanerjee S, Magnani E, Ukomadu C, Lujambio A, Bernstein E, Sadler KC (2019) Epigenetic Compensation Promotes Liver Regeneration. *Dev Cell* 50: 43-56 e46
Yang L, Wang X, Yu XX, Yang L, Zhou BC, Yang J, Xu CR (2023) The default and directed pathways of hepatoblast differentiation involve distinct epigenomic mechanisms. *Dev Cell* 58: 1688-1700 e1686
Zhang C, Macchi F, Magnani E, Sadler KC (2021) Chromatin states shaped by an epigenetic code confer regenerative potential to the mouse liver. *Nat Commun* 12: 4110
Zhao Y, Guan YY, Zhao F, Yu T, Zhang SJ, Zhang YZ, Duan YC, Zhou XL (2022) Recent strategies targeting Embryonic Ectoderm Development (EED) for cancer therapy: Allosteric inhibitors, PPI inhibitors, and PROTACs. *Eur J Med Chem* 231: 114144

Figure 1.

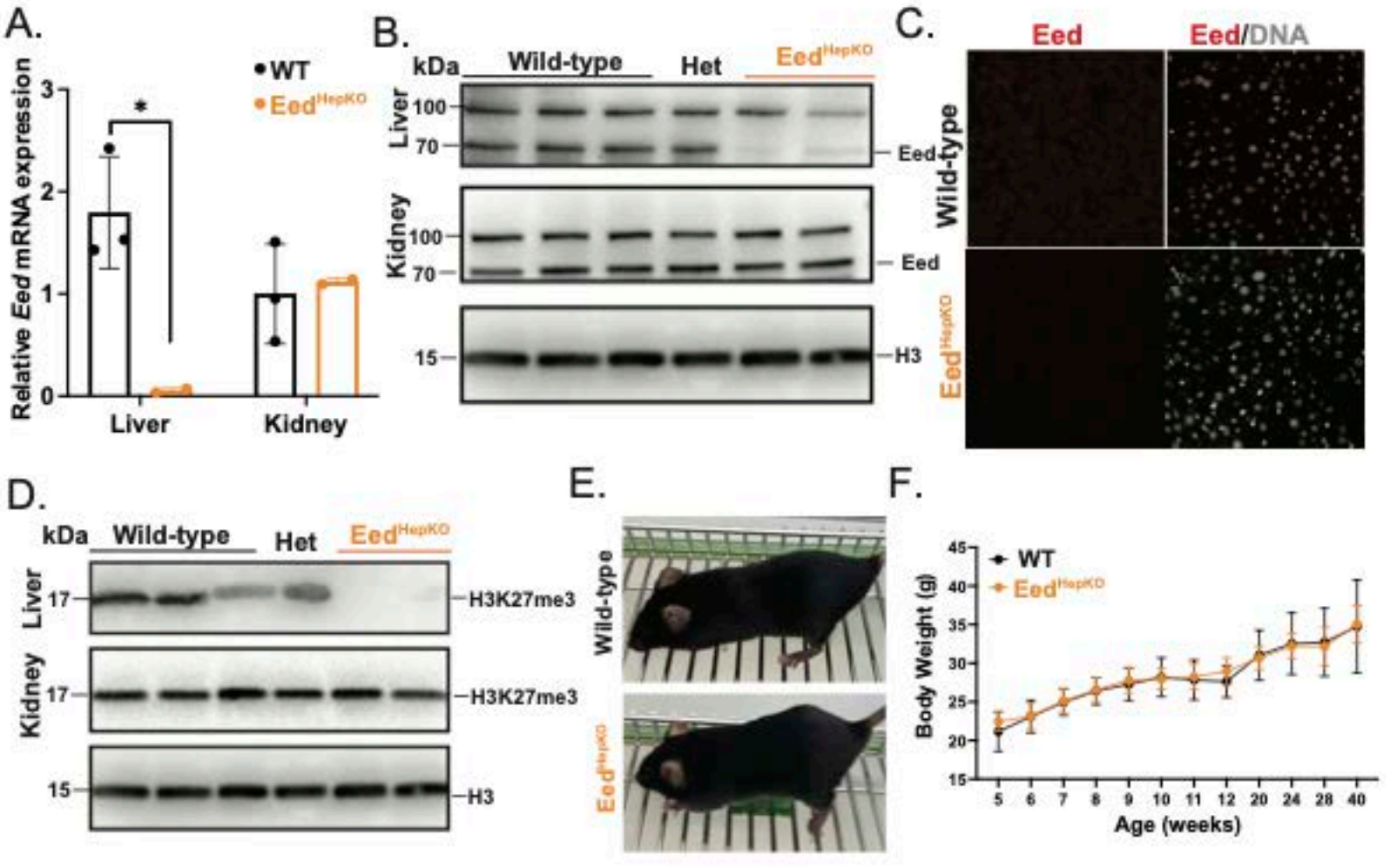
A.
WT
Eed HepKO
Relative Eed mRNA expression
3
2
1
0
*
Liver
Kidney
B.
kDa
Wild-type
Het
Eed HepKO
Liver
100
70
Eed
Kidney
100
70
Eed
15
H3
C.
Eed
Eed/DNA
Wild-type
Eed HepKO
D.
kDa
Wild-type
Het
Eed HepKO
Liver
17
H3K27me3
Kidney
17
H3K27me3
15
H3
E.
Wild-type
Eed HepKO
F.
WT
Eed HepKO
Body Weight (g)
45
40
35
30
25
20
15
5
6
7
8
9
10
11
12
20
24
28
40
Age (weeks)

Figure 2.

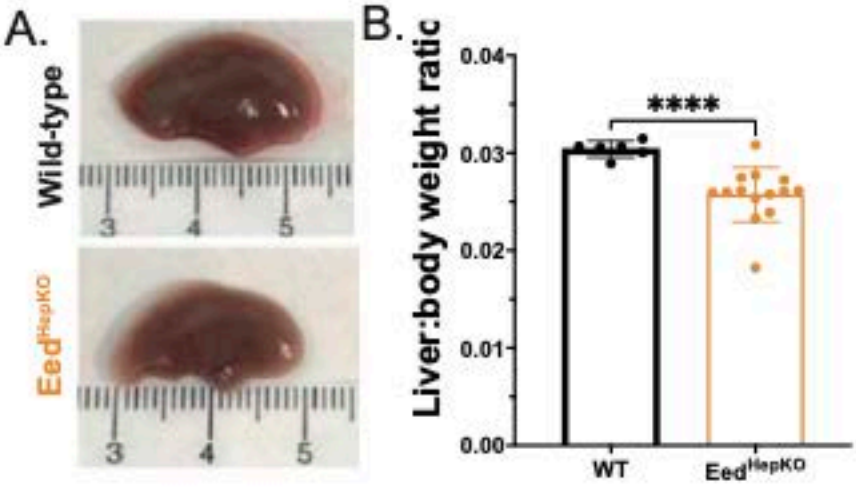

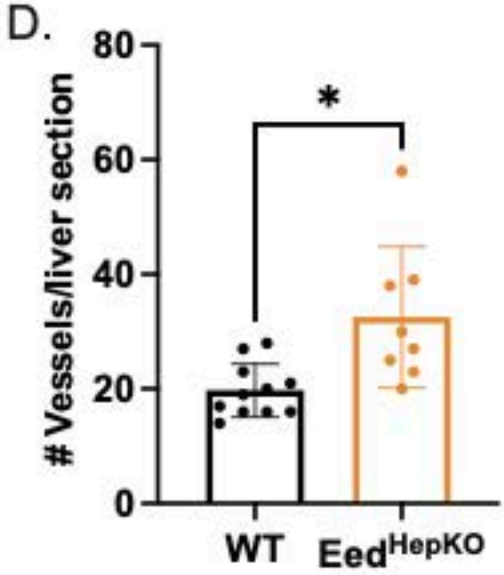

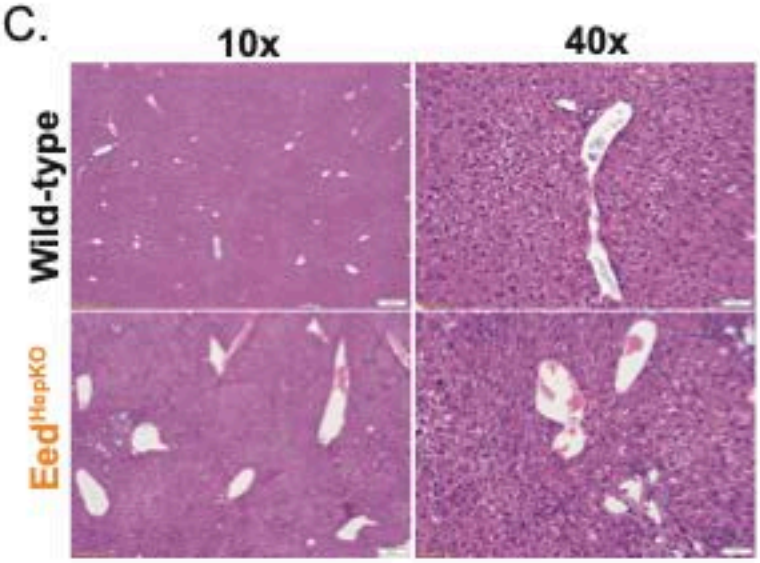

E.

	WT	Eed^HepKO
Biliary Fibrosis	0/5	1/5
Ductular Reaction	0/5	1/5
Cell Death	0/5	0/5
Proliferation	0/5	1/5
Inflammation	0/5	3/5

Figure 3 .

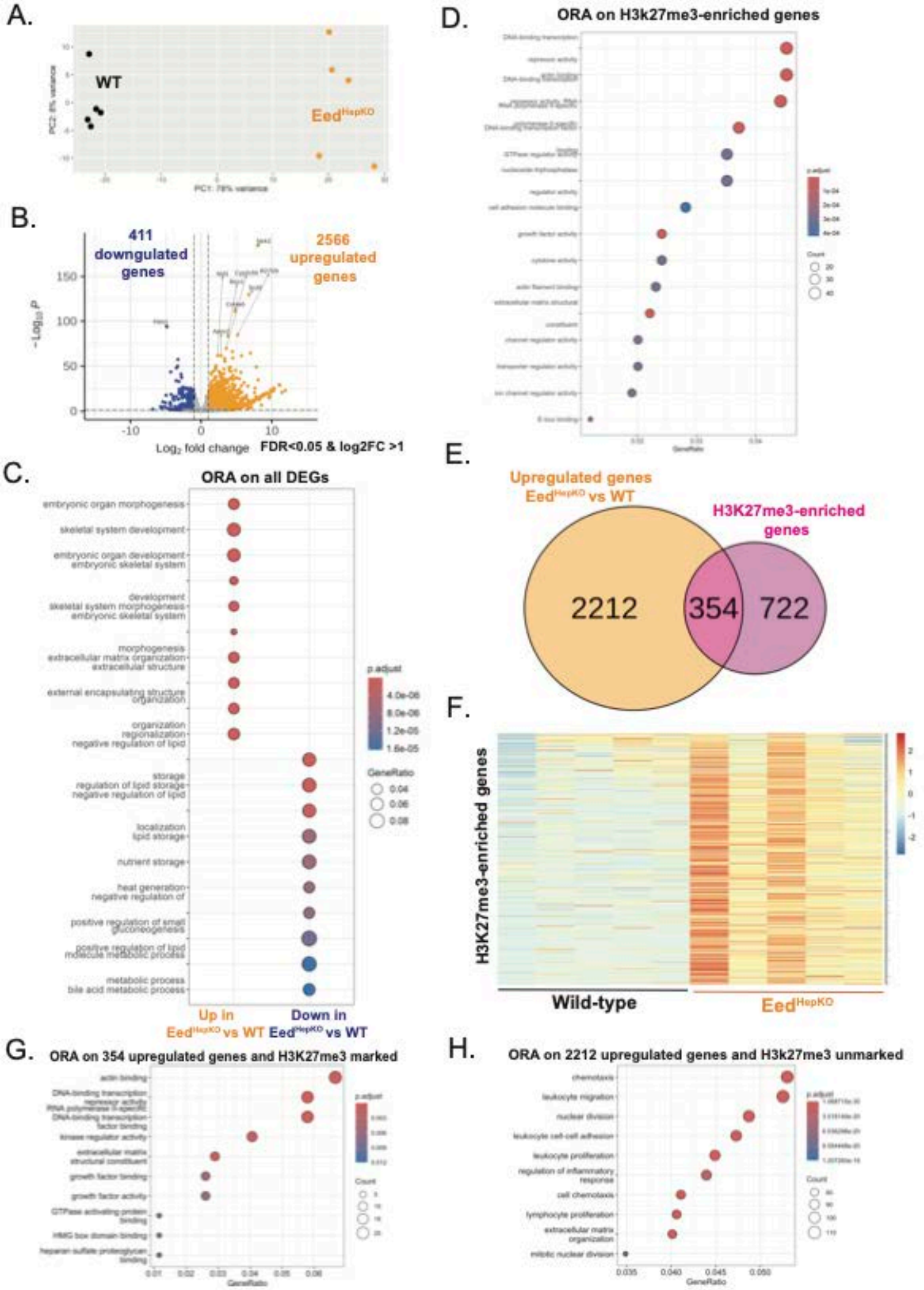
A.
WT
Eed^HepKO
PC2: 8% variance
PC1: 78% variance
B.
411 downgulated genes
2566 upregulated genes
−Log10 P
Log2 fold change
FDR<0.05 & log2FC >1
C.
ORA on all DEGs
embryonic organ morphogenesis
skeletal system development
embryonic organ development
embryonic skeletal system
development
skeletal system morphogenesis
embryonic skeletal system
morphogenesis
extracellular matrix organization
extracellular structure
external encapsulating structure organization
organization
regionalization
negative regulation of lipid
storage
regulation of lipid storage
negative regulation of lipid
localization
lipid storage
nutrient storage
heat generation
negative regulation of
positive regulation of small gluconeogenesis
positive regulation of lipid molecule metabolic process
metabolic process
bile acid metabolic process
Up in Eed^HepKO vs WT
Down in Eed^HepKO vs WT
p.adjust
GeneRatio
D.
ORA on H3k27me3-enriched genes
E.
Upregulated genes Eed^HepKO vs WT
H3K27me3-enriched genes
2212
354
722
F.
H3K27me3-enriched genes
Wild-type
Eed^HepKO
G.
ORA on 354 upregulated genes and H3K27me3 marked
actin binding
DNA-binding transcription repressor activity
RNA polymerase II-specific
DNA-binding transcription factor binding
kinase regulator activity
extracellular matrix structural constituent
growth factor binding
growth factor activity
GTPase activating protein binding
HMG box domain binding
heparan sulfate proteoglycan binding
p.adjust
Count
GeneRatio
H.
ORA on 2212 upregulated genes and H3k27me3 unmarked
chemotaxis
leukocyte migration
nuclear division
leukocyte cell-cell adhesion
leukocyte proliferation
regulation of inflammatory response
cell chemotaxis
lymphocyte proliferation
extracellular matrix organization
mitotic nuclear division
p.adjust
Count
GeneRatio

Figure 4.

A.

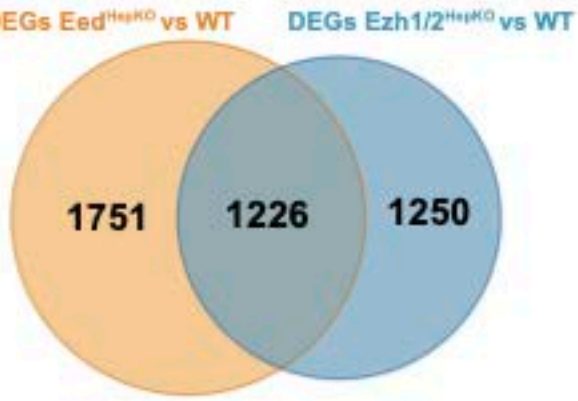

B.

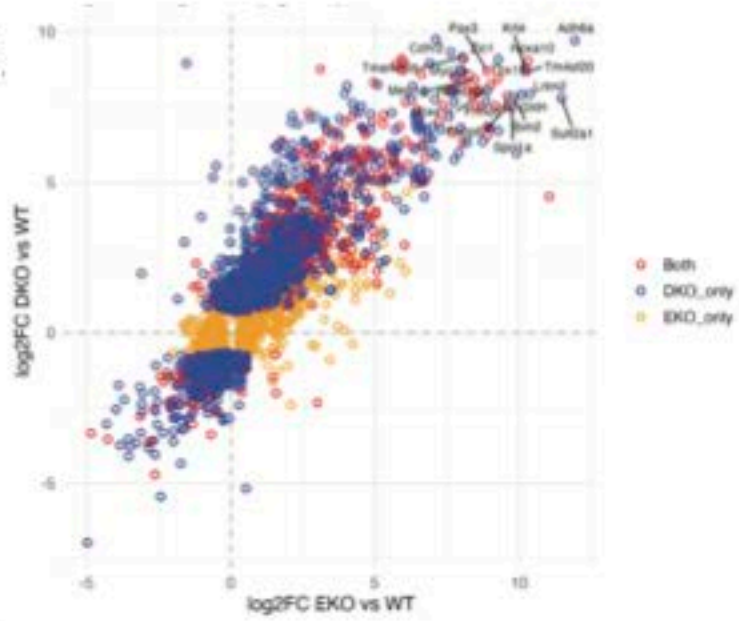

C

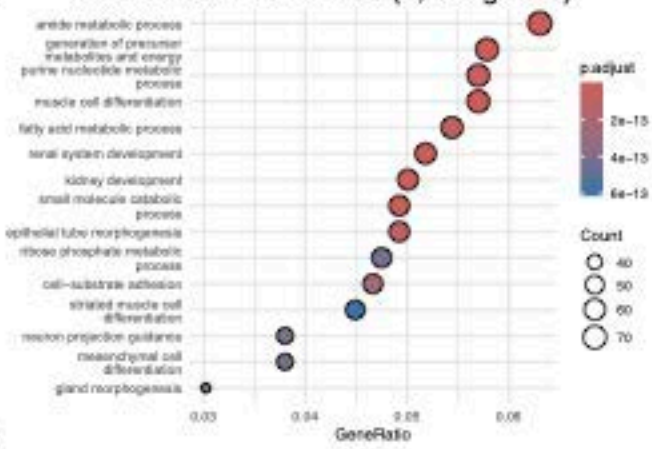

D.

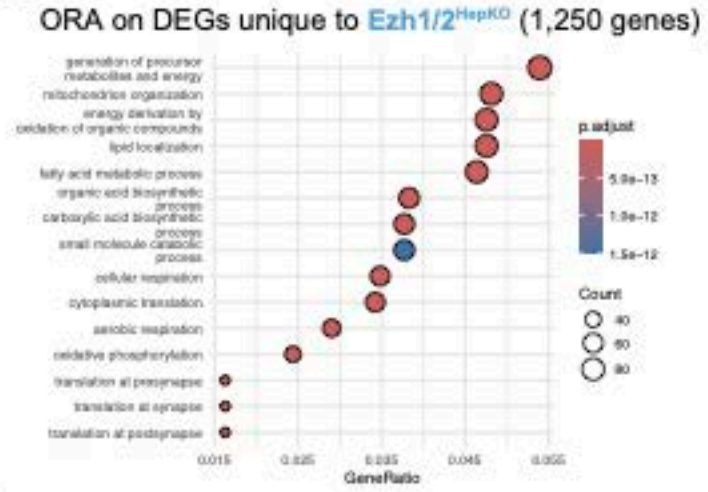

E.

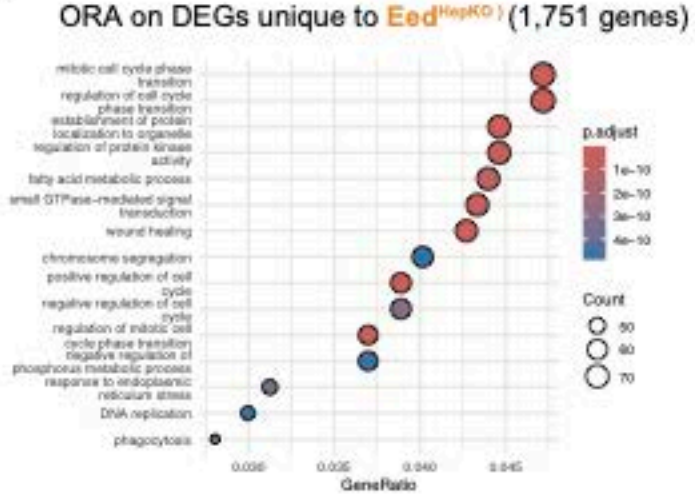

F.

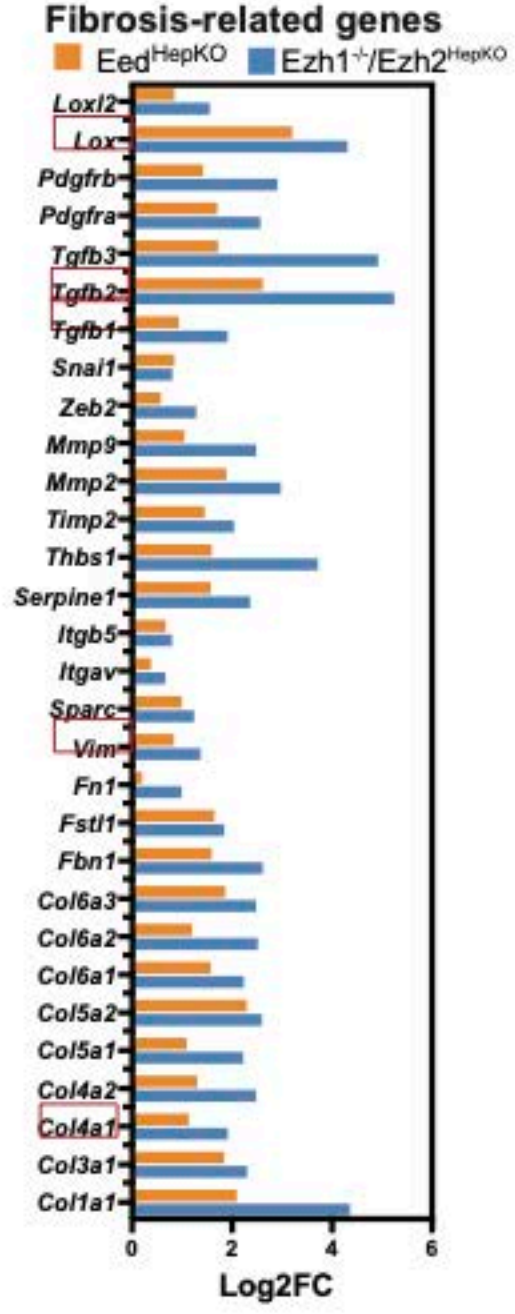

Figure 5.

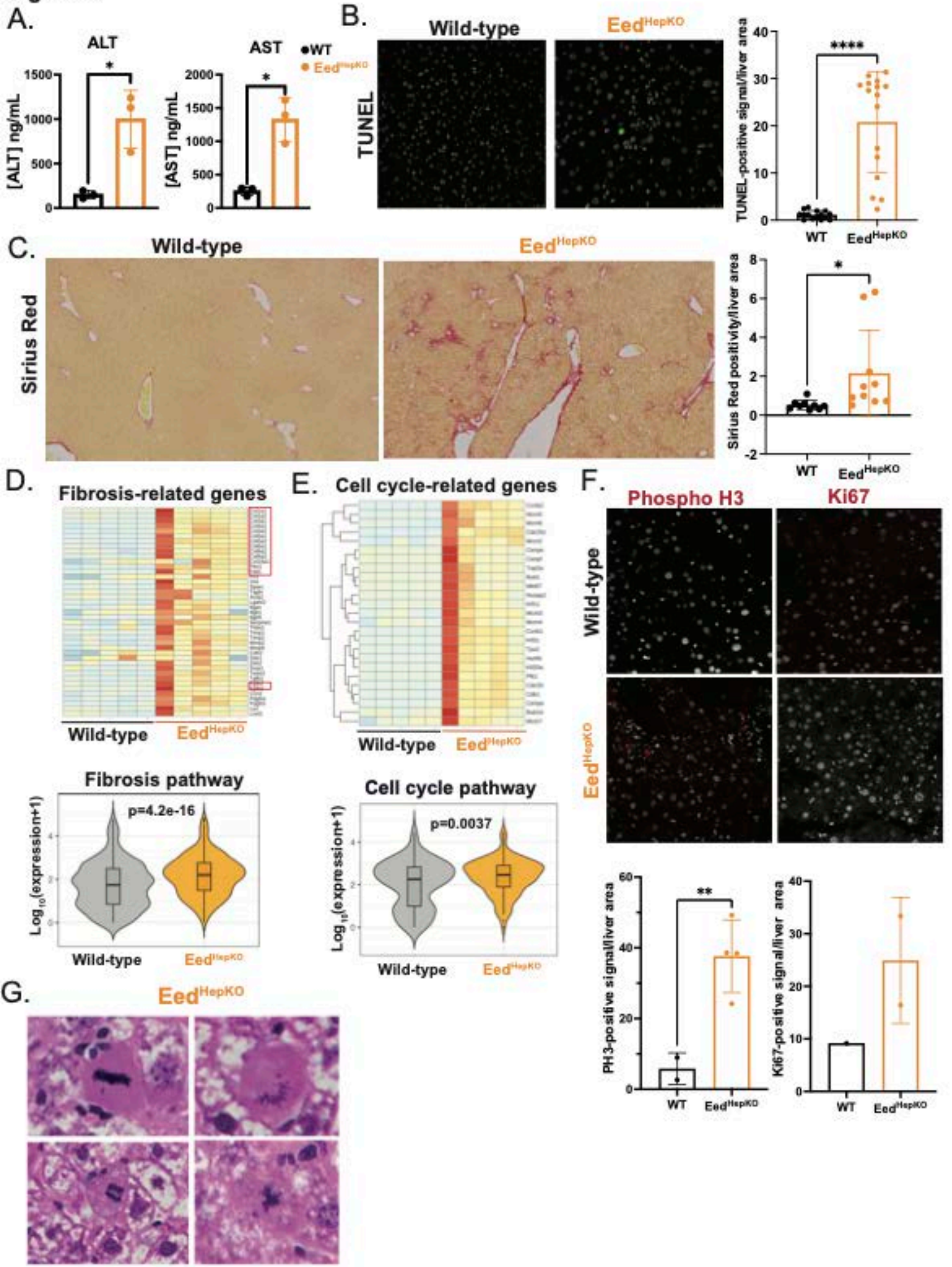
A.
ALT
AST
●WT
● Eed^HepKO
[ALT] ng/mL
[AST] ng/mL
B.
Wild-type
Eed^HepKO
TUNEL
TUNEL-positive signal/liver area
****
WT
Eed^HepKO
C.
Wild-type
Eed^HepKO
Sirius Red
Sirius Red positivity/liver area
*
WT
Eed^HepKO
D.
Fibrosis-related genes
Wild-type
Eed^HepKO
Fibrosis pathway
p=4.2e-16
Log10(expression+1)
Wild-type
Eed^HepKO
E.
Cell cycle-related genes
Wild-type
Eed^HepKO
Cell cycle pathway
p=0.0037
Log10(expression+1)
Wild-type
Eed^HepKO
F.
Phospho H3
Ki67
Wild-type
Eed^HepKO
PH3-positive signal/liver area
**
Ki67-positive signal/liver area
WT
Eed^HepKO
G.
Eed^HepKO

Figure 6.

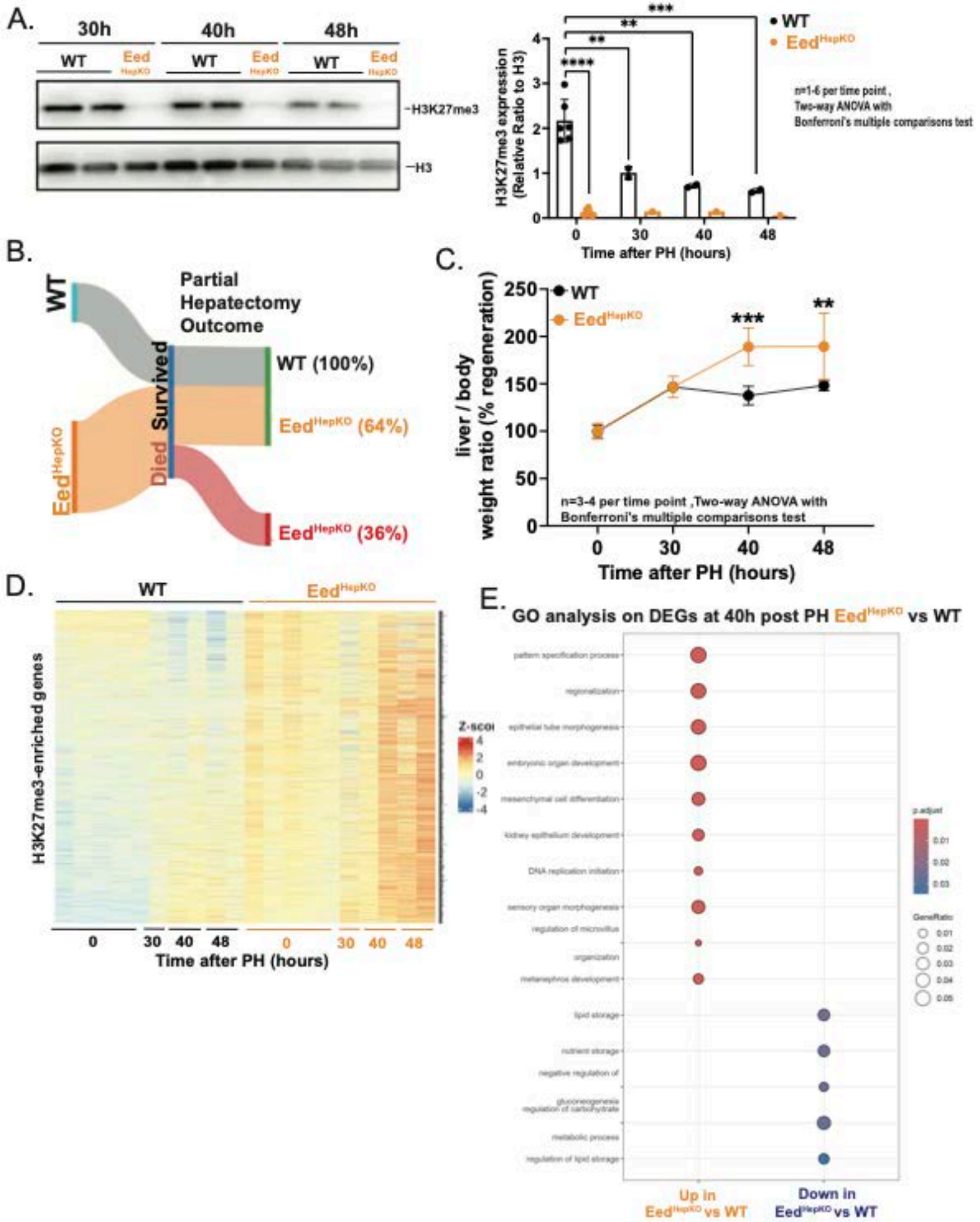
A.
30h
40h
48h
WT
Eed HepKO
H3K27me3
H3
H3K27me3 expression (Relative Ratio to H3)
Time after PH (hours)
n=1-6 per time point , Two-way ANOVA with Bonferroni's multiple comparisons test
B.
Partial Hepatectomy Outcome
Survived
Died
WT (100%)
Eed HepKO (64%)
Eed HepKO (36%)
C.
liver / body weight ratio (% regeneration)
n=3-4 per time point ,Two-way ANOVA with Bonferroni's multiple comparisons test
D.
H3K27me3-enriched genes
Z-score
E.
GO analysis on DEGs at 40h post PH Eed HepKO vs WT
pattern specification process
regionalization
epithelial tube morphogenesis
embryonic organ development
mesenchymal cell differentiation
kidney epithelium development
DNA replication initiation
sensory organ morphogenesis
regulation of microvillus organization
metanephros development
lipid storage
nutrient storage
negative regulation of gluconeogenesis
regulation of carbohydrate metabolic process
regulation of lipid storage
p.adjust
GeneRatio
Up in Eed HepKO vs WT
Down in Eed HepKO vs WT